Chapter

Recent Advances in Diamond Radiation Detectors for Extreme Environments: A Review

YunPeng Yang, Sen Zhang, Benjian Liu, Zuanquan Chen, Rui Fan, Chao Chen, Linlin Liu, Wensi Yang, Binyu Niu, Rui Chen, Tao Li, Kang Liu, Bing Dai and Jiaqi Zhu

Abstract

Diamond has emerged as a highly promising ultra-wide bandgap semiconductor for radiation detection, especially in extreme environments where conventional materials prove ineffective. Its high carrier mobility, outstanding radiation resistance, and remarkable thermal and structural stability render it a prime candidate for next-generation detectors. Owing to advancements in chemical vapor deposition (CVD) techniques, high-quality single-crystal diamond can now be produced with enhanced reproducibility, facilitating more advanced device designs. Innovations like metal nanoparticle-embedded nanowire structures and hetero-integrations with 2D materials have exhibited substantial improvements in sensitivity and response stability for applications such as solar-blind UV detection and X-ray imaging. Furthermore, diamond-based detectors have demonstrated reliable operation at temperatures reaching up to 425°C and under high neutron fluence, highlighting their potential for utilization in challenging conditions, including deep space exploration, nuclear reactor monitoring, and long-term energy storage systems. Although challenges persist in terms of scaling and cost-effective manufacturing, the unique performance advantages of diamond indicate an increasingly significant role in future high-performance detection technologies.

Keywords: diamond, radiation detectors, high energy physics, high temperature operation, beam monitor

1. Introduction

As an ultra-wide bandgap semiconductor material (with a bandgap width of 5.47 eV), diamond has drawn extensive attention in the field of radiation detection in recent years [1]. Its distinctive physicochemical properties, such as high carrier mobility (exceeding 2000 cm^2V^{-1} s^{-1}), a high breakdown electric field (exceeding 10 MV/cm),

strong radiation resistance, and the highest thermal conductivity among all known materials (22 W/cm·K), render it an ideal choice for radiation detection in extreme environments. Compared with traditional silicon-based and germanium-based detectors, diamond detectors exhibit lower dark current, faster time response, and stronger environmental adaptability. They can operate stably under harsh conditions like high temperature and high radiation. In recent years, with the advancement of chemical vapor deposition (CVD) technology, the production of high-quality single crystal diamonds has become feasible, which has spurred the rapid development of diamond radiation detectors [2, 3].

Currently, the research on diamond radiation detectors has transitioned from the preparation of basic materials to the design and application of devices, and it has demonstrated significant potential in areas such as deep-space exploration, nuclear reactor monitoring, high-energy physics experiments, and biomedical imaging. Particularly in cutting - edge fields like high-temperature deep-ultraviolet detection, high-resolution energy spectroscopy analysis, and radiation-resistant particle monitoring, diamond detectors have achieved performance breakthroughs that traditional semiconductor detectors find difficult to attain. This chapter will systematically review the latest research progress of diamond radiation detectors from five aspects: materials and device engineering, detection performance breakthroughs, adaptability to extreme environments, expansion of application scenarios, and future challenges, offering a comprehensive reference for researchers and technology developers in related fields.

2. Progress in materials and device engineering

The performance enhancement of diamond radiation detectors primarily stems from innovative breakthroughs in material preparation and device structure. Optimizing single-crystal diamond materials is fundamental to detector performance. Through advanced CVD technology, researchers have managed to prepare high-purity single-crystal diamond substrates with extremely low defect densities ($<10^{15}$ cm^{-3}). At a 150 V bias, the dark current density of these substrates can be controlled below 0.26 pA/mm^2. The charge collection efficiencies of electrons and holes are as high as 98.9 and 99.2%, respectively, and the energy resolution reaches an excellent level of 2.54–2.86%. The research team at Rio de Janeiro University of Technology further eliminated diamond surface defects via a thermochemical treatment process, boosting device performance by 10–15% compared to traditional solutions.

Nanostructure design has emerged as a crucial approach for enhancing the performance of diamond detectors. The embedded platinum nanoparticle single-crystal diamond nanowire structure developed by the Institute of Metals of the Chinese Academy of Sciences ingeniously combines the outstanding carrier transport ability of one-dimensional nanowires with the local surface plasma resonance effect of platinum nanoparticles. This structure exhibits a response of 68.5 A/W under 220 nm ultraviolet light, which is over 2000 times higher than that of traditional bulk diamond devices. Even more remarkable is that when the temperature rises to 275°C, the response further soars to 3098.7 A/W, and the ultraviolet/visible suppression ratio reaches as high as 4303. This effectively resolves the issue of deterioration of the oxygen terminal structure at high temperatures.

Heterogeneous integration and interface engineering pave the way for new directions for diamond detectors. The research team from the National University of Defense Technology innovatively employed the Van der Waals heterojunction bonding technology to integrate few-layer graphene and hexagonal boron nitride (h-BN) with a diamond substrate, constructing a diamondene photodetector featuring an interfacial bonding structure. This structure exhibits a response of 2.04 A/W in the 230 nm band, which is 45 times faster than that of conventional diamond detectors. It has a detection rate exceeding 10^{12} Jones and an ultra-low light imaging capability of merely 28 photons. This heterostructure effectively overcomes the inherent drawback of insufficient free electron concentration in diamonds and offers a new model for ultra-high sensitivity detection.

At the "electronic design" level, a significant breakthrough has also been achieved in the dedicated readout circuit for diamond detectors. The newly developed low-noise, high-gain charge-sensitive amplifier employs a combined design of a common source pole amplifier and a differential amplifier, attaining a background equivalent noise charge (ENC) of 168 e^-. It has a charge collection efficiency of 86% and a spectral resolution of 2.63%, which notably enhances the signal extraction capability of the diamond detector. This low-noise design paves the way for diamond detectors in high-precision spectral analysis and beam current monitoring.

2.1 Comparison of HPHT and CVD diamond detector performance

Crystal mass is a crucial parameter influencing the performance of diamond detectors [4], and the quality of homogeneously epitaxially grown diamonds largely hinges on the substrate quality. Currently, remarkable progress has been achieved in synthesizing high-quality millimeter-thick single-crystal diamonds using high-temperature and high-pressure (HPHT) and plasma-assisted CVD techniques. The HPHT method has produced type IIa high-purity crystals with low defect density. This offers higher detection accuracy and reliability for the application of diamond nuclear radiation detectors and broadens their extensive application prospects in nuclear energy, medical imaging, and nuclear materials research. However, new dislocations are generated during CVD growth, with a dislocation density of approximately 10^3–10^5 cm^{-2}. Nevertheless, CVD diamonds generally have lower impurity content compared to HPHT seed crystals.

Through the design of a microwave chemical vapor deposition chamber integrated with plasma purification technology, high-purity single crystal diamonds were epitaxially grown. Trace substituted nitrogen impurities in the diamonds were characterized using electron paramagnetic resonance, revealing extremely low impurity concentrations (2.1 ppb) in the CVD diamonds. The energy resolutions of the HPHT single crystal and CVD diamond detectors for alpha particles were 2.04 and 0.86%, respectively. Based on Schottky characteristics and defect regulation, the CVD diamond detector achieves a self-bias spectral response to alpha particles, with its charge collection efficiency (CCE) reaching 10.76%. Under high bias voltage, the CCEs of the HPHT single crystal and CVD diamond detectors were 38.11 and 86.65%, respectively. The relatively lower CCE of the HPHT diamond detector is primarily due to the deep trapping effect of substituted nitrogen impurities on carriers. The spatial polarization effect caused by dislocations results in the formation of an electric field within the detector, which is the main factor influencing carrier transport in CVD diamonds.

3. Breakthrough in detection performance

3.1 Sunblind UV detector

The ideal sunblind UV detector should not only possess excellent spectral selectivity but also be capable of operating stably in extreme environments like high temperatures. Jiaqi Lu et al. proposed a single crystal diamond nanowire structure embedded with platinum nanoparticles [5], as depicted in **Figure 1**. This structure integrates the outstanding carrier transport capability of one-dimensional nanowires, the local surface plasmon resonance effect of platinum nanoparticles, the local Schottky barrier at the platinum/diamond interface, and the photoelectric gain mechanism induced by deep energy traps at high temperatures. It demonstrates remarkable advantages in enhancing the efficiency of light absorption, carrier generation, and separation, thereby significantly improving the photoelectric response ability of oxidizing terminal diamonds at high temperatures. The response of the device fabricated with this material reaches 68.5 A/W, which is approximately 2000 times higher than that of traditional oxygen-terminal block diamond devices, and the UV/Vis rejection ratio is 550 (**Figure 2**).

Additionally, Chao-Nan Lin et al. fabricated a diamond photodetector featuring a MEMS structure [6]. By creating hydrogen terminals on the diamond surface, they managed to lower the height of the Schottky barrier at the gold/diamond contact interface (**Figure 3**). The detector exhibits a remarkable response rate of up to 524.9 A/W

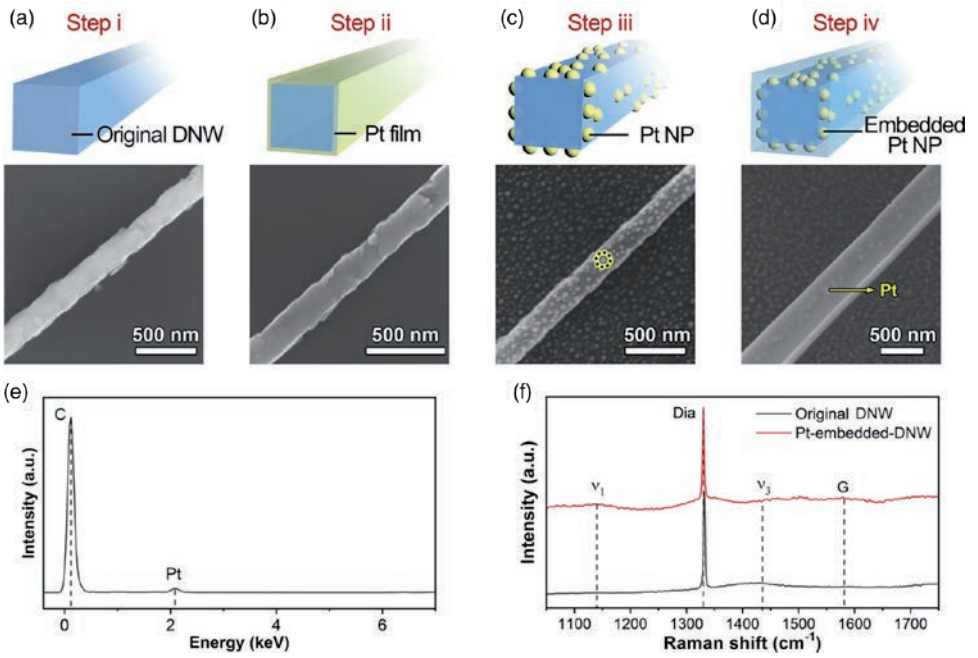


Figure 1.
Fabrication of Pt nanoparticles-embedded DNWs through a four-step process: (a) Step i: Preparation of the original DNWs via deposition of a [001]-orientated micro–/nanograin diamond film and thermal oxidation. (b) Step ii: Deposition of a 2-nm Pt film on the surface of the DNWs. (c) Step iii: Dewetting of the Pt film into nanoparticles by MPCVD. (d) Step iv: Diamond homoepitaxial regrowth by MPCVD to form Pt-embedded DNWs. SEM images corresponding to each step are presented in the figure. (e) EDS spectrum collected from the yellow dotted regions in (c). (f) Raman spectra of the DNWs before and after Pt embedding and diamond homoepitaxial growth [5]. Copyright 2025, published by Springer Nature, used with permission of the publisher.

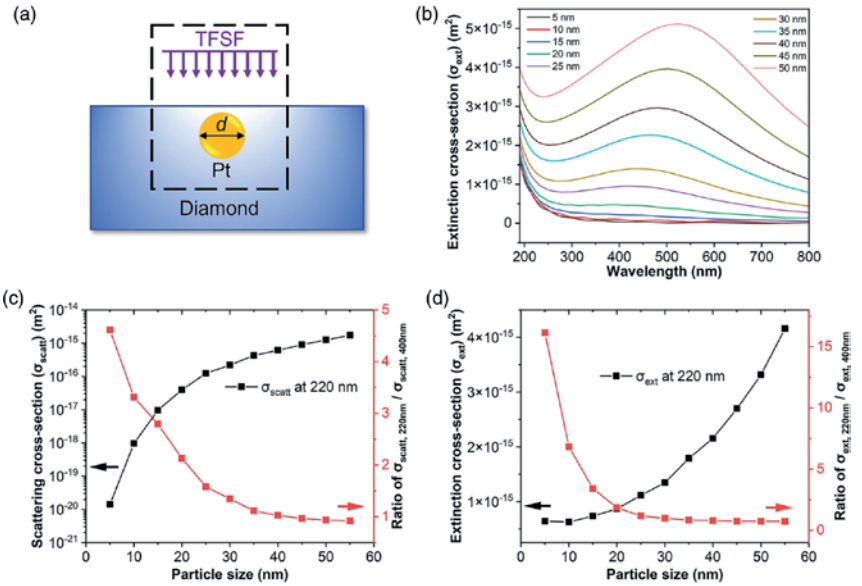


Figure 2.
(a) Schematic illustration of the model employed for FDTD simulations; (b) spectral extinction cross-sections for diverse Pt nanoparticle sizes; (c) scattering cross-section and (d) extinction cross-section as a function of Pt nanoparticle size: the black curve depicts the cross-sections at 220 nm, and the red curve represents the ratio of the cross-sections at 220 nm to those at 400 nm [5]. Copyright 2025, The Authors, published by Springer Nature, used with permission of the publisher.

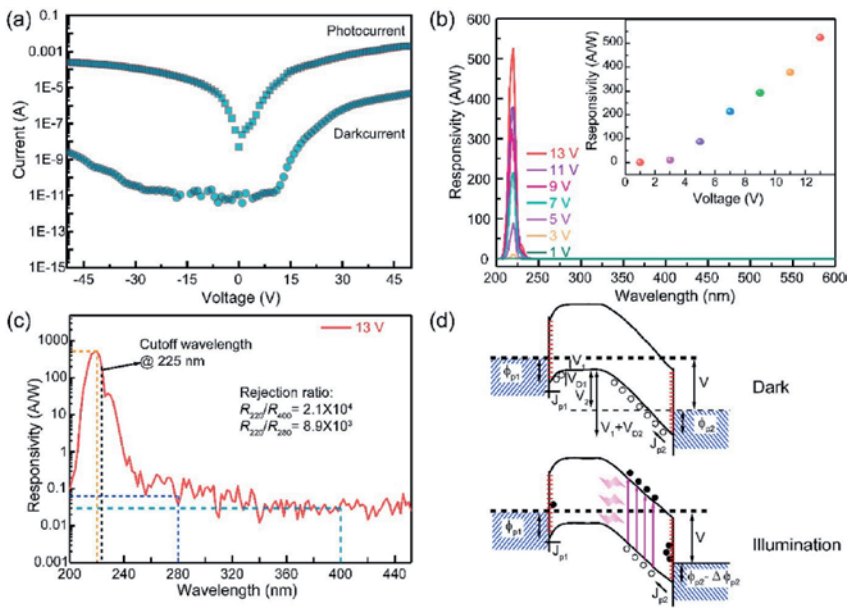


Figure 3.
(a) I–V curves of the diamond MSM photodetector in the dark (circles) and under UV illumination (squares). (b) The spectral responsivity of the photodetector at different applied voltages. The inset shows the peak responsivity under biases ranging from 1 to 13 V. (c) The plot of the response responsivity at a 13 V bias on a semi-logarithmic scale. (d) Schematic of the energy diagram of the Au/hydrogenated diamond/Au photodetector in the dark and under UV illumination [6]. Copyright 2022, Elsevier, used with permission of the publisher.

and a detection rate reaching as high as 3.42 × 1015 cm $Hz^{1/2}$ W^{-1}. This achievement offers a novel approach for high-performance diamond solar-blind UV photodetectors.

3.2 X-ray detector

Dou Wenjie and others employed single crystal diamond to build an X-ray detector array (**Figure 4**). They enhanced the detector's sensitivity via an asymmetric sandwich electrode structure. The detector demonstrates a light-dark current ratio of 18,312, a sensitivity of 14.3 mC Gy^{-1} cm^{-2}, and a detection limit of 4.9 nGy s^{-1} at a 50 V bias, attaining the best level among current diamond X-ray detectors [7].

The surface modification of hydrogen-terminated diamond (H-diamond) has been employed to optimize diamond devices [8–11]. Specifically, superior ohmic contact can be attained on H-diamond by using high work function metals (such as Au) because of the appropriate work function and negative electron affinity (−0.4 to −1.3 eV) of the H-diamond surface [12, 13]. Therefore, it can be expected that the electrode contact with H-diamond surface modification will optimize the DRD for medical applications and simplify the electrode complexity when compared with the multilayer electrode structure, *in-situ* doping, and ion implantation processes [14]. Some scholars have reported for the first time the dose detection characteristics of DRD with an Au/H-diamond electrode for X-rays. The large gain, high sensitivity, and linearity of the device for X-ray dose detection, as well as the energy resolution for an α - source, are demonstrated.

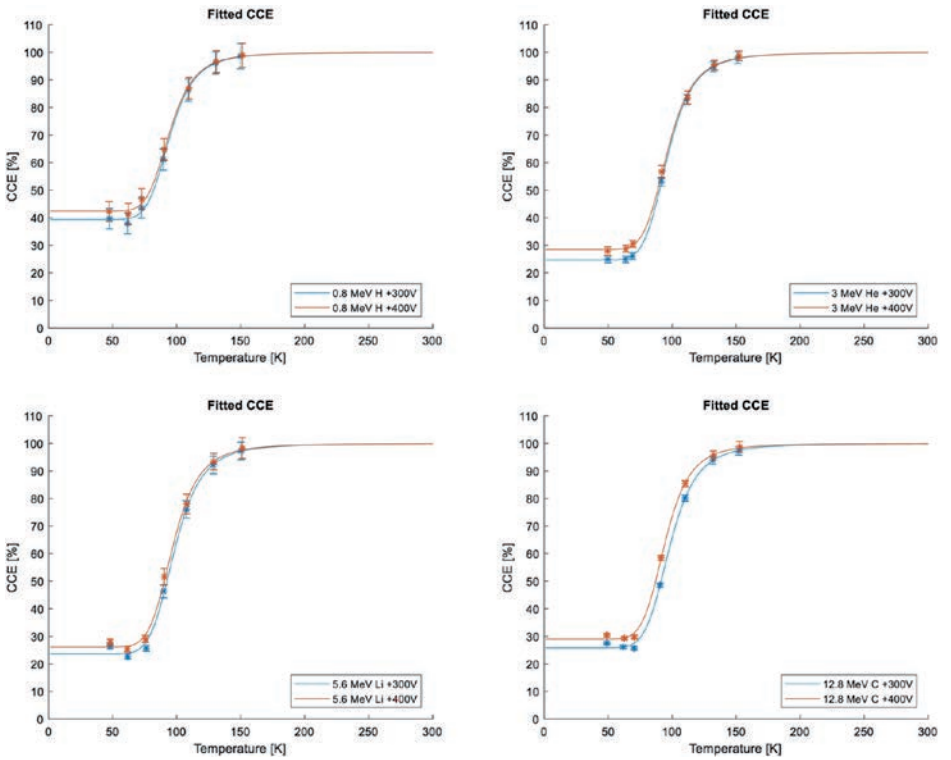


Figure 4.
Influence of the detector bias on the CCE. Copyright 2022, Elsevier, used with permission of the publisher.

3.3 Construction of novel electrodes

Rebecca et al. employed laser writing technology to significantly enhance the resolution and charge collection efficiency of the detector by introducing nanocarbon network electrodes on diamond substrates [1]. First, a two-dimensional spiral NCN wire was fabricated using a pulsed fs laser. The writing process commences 20 μm beneath the surface and constructs layer by layer to create a wall with a height of 20 μm, reaching the top surface (**Figure 5**). This depth was selected to match the penetration depth of the test alpha particles. When designing a detector for other types of more penetrating radiation, it is feasible to increase the wall depth. Furthermore, it is anticipated that in the future, the internal NCN electrodes could be connected via the back of the substrate using NCN through vias. This would allow for the removal of metal contacts from the alpha-facing surface, which is a known weak point for detectors exposed to large doses of gamma radiation 30.

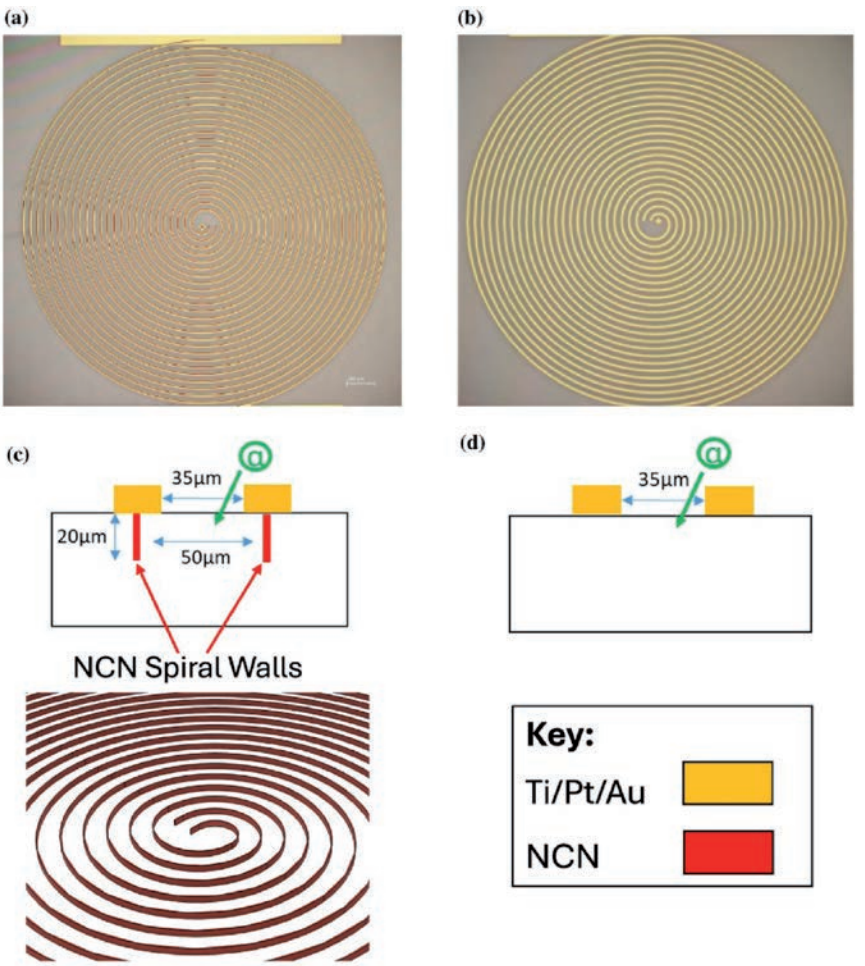


Figure 5.
Optical microscope images of the fabricated spiral detectors with and without internal nano-carbon network "wall" electrodes (a and b), as well as a side cross-section (c and d). Copyright 2025, The Authors, published by Springer Nature, used with permission of the publisher.

4. Suitability for extreme environments

4.1 Mixed radiation fields

The single-crystal chemical vapor deposition (CVD) diamond detectors (SDDs) assembled with detector-grade single-crystal diamonds (SCDs) are commercially available [15]. It is usually less than 10 cm^3, including the detector housing [16]. Some studies have shown that the detection efficiency of SDDs for 14-MeV neutrons remains stable up to a neutron fluence of approximately 0.5×10^{14} n cm^{-2} (**Figure 6**) [17].

It has demonstrated the high-temperature tolerance of SDDs in neutron measurement at temperatures up to 473 K [18]. These excellent characteristics of SDDs should allow for neutron measurement in harsh environments within advanced systems. An evaluation of the neutron energy spectrum by combining pulse shape discrimination (PSD) processing to extract pulses induced solely by fast neutrons in the SDD has been raised. This method includes processes to reject pulses induced by gamma rays and energetic ions during PSD processing and has demonstrated reliable quantitative evaluation capabilities for the neutron energy spectrum. Consequently, the developed method enables the measurement of fast neutrons in a mixed radiation field [19].

4.2 Operation of diamond detectors under extreme temperature conditions

The reliability of radiation detectors under extreme temperatures serves as a crucial indicator of their performance. For instance, radiation detectors must maintain stable performance in high-temperature settings for radiation monitoring near engine combustion chambers or on high - speed aircraft surfaces, or for the monitoring and imaging of radioactive materials in metallurgical and glass manufacturing processes. Numerous cutting edge physics experiments (such as quantum computing and dark matter detection) usually operate at extremely low temperatures. These experiments demand sensors for *in-situ* radiation monitoring. Diamond detectors are anticipated to have a role in the detection system of the Large Particle Collider, where some components operate at low temperatures to reduce noise. Low-temperature environments (like nuclear fusion reactors) place extremely high demands on detector performance. Therefore, it is essential to conduct further research on the performance of diamond detectors at low temperatures. D. Cosic et al. investigated the charge collection efficiency of electron-scale single crystal chemical vapor deposition diamond detectors and measured it using four ions with MeV

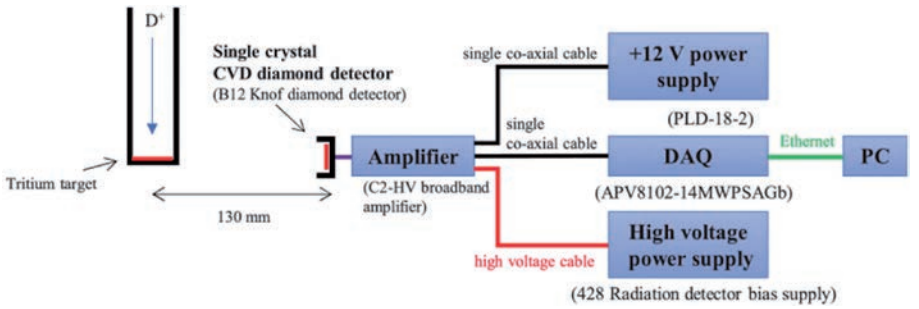


Figure 6.
Schematic diagram of (a) the detector layout during 14.1-MeV neutron irradiation, (b) the detector layout during 5.5-MeV neutron irradiation, and (c) the layout of electronic components employed in both experiments. Copyright 2024, IEEE, used with permission of the publisher.

energies from room temperature down to 47 K. For different ions, the detector's charge collection efficiency (CCE) exhibits a similar trend with temperature. One plateau was observed from room temperature to 145 K, followed by a sharp decline from 65 to 145 K [20]. Below 65 K, the CCE reached another plateau (**Figure 4**). Within the same temperature range, the charge collection efficiency of each ion decreases.

Regarding the performance research of diamond detectors at high temperatures, certain scholars have designed and fabricated a prototype of an 8 pixel diamond detector with a tungsten electrode that operates at high temperatures. The tungsten electrode of the designed detector exhibits ohmic contact with the diamond, which verifies that it is a suitable contact material for diamond detectors at high temperatures (**Figure 7**). Under a thermal stress cycle lasting 330 hours, the detector's dark current demonstrated stable repeatability, and the photocurrent signal under X-ray also showed excellent repeatability.

Additionally, certain scholars have investigated the performance of artificial monocrystalline CVD diamond detectors operating in current mode at high temperatures (HT) [22]. First, the leakage current of the detector was characterized in relation to temperature and bias voltage (HV). Subsequently, the detector was exposed to intense 60Co gamma-ray fluxes. Its response to the "normalized current" (defined here as the measuring current minus the leakage current, normalized to the gamma dose rate or gamma flux) and its time-dependent behavior were studied within a temperature range from 300 K (room temperature) to 625 K. The detector response exhibits a linear response to HV with dose rates up to approximately 600 K (**Figure 8**). At higher temperatures, the saturation of the measured net current is observed, along with the polarization effect.

4.3 Radiation hardness

Commercial high-purity single-crystal diamond detectors have been thoroughly investigated using focused ion beams (carbon, hydrogen, helium, and other ions) within the MeV energy range. The measurement for detecting 2 MeV protons has

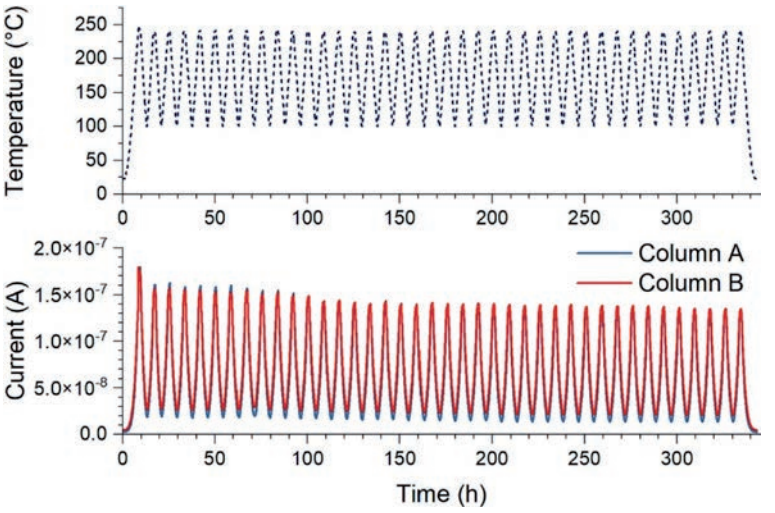


Figure 7.
Dark current measurements as a function of temperature and time: Evolution of current for the two columns of pixels during 40 thermal cycles (with a total duration of 330 h), where the temperature was maintained between 100 and 240°C [21]. Copyright 2023, Elsevier, used with permission of the publisher.

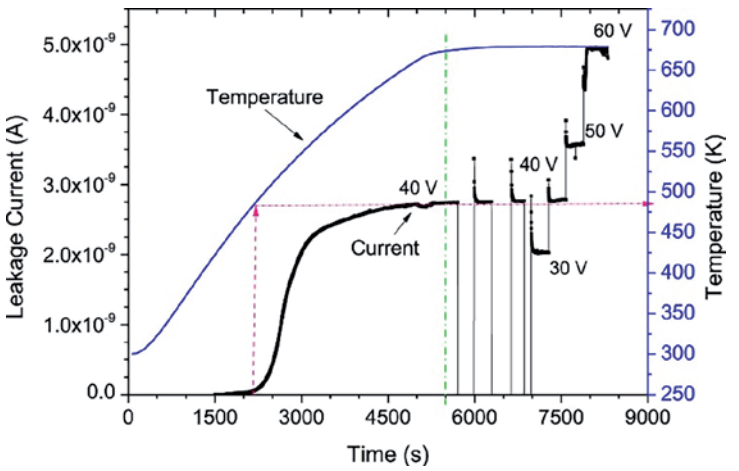


Figure 8.
Measured leakage current (black curve, left axis) during the diamond detector heating up to 675 K; the temperature increase is also presented (blue curve, right axis). The red arrows denote the temperature (480 K) above which the leakage current begins to rise. The plot also illustrates the detector's behavior when the bias voltage is switched on/off and when its value is changed in a stepwise increase/decrease manner [22]. Copyright 2019, Elsevier, used with permission of the publisher.

a relative energy resolution of 1.3% (FWHM = 25 KeV), suggesting that the CVD diamond device possesses excellent spectral performance, rendering it useful for detecting light ions or atoms. The radiation hardness of a particle detector is a crucial parameter for complex detector systems employed in high-energy physics. Previous studies have demonstrated that CVD diamond detectors display superior radiation hardness compared to standard silicon-based detectors when detecting high-energy particles. To assess the radiation hardness of diamond detectors, researchers selectively irradiated them with a 6.5 MeV focused carbon beam with a flux of up to 10^{11} ions/cm^2. Reliable measurement of ion flux is accomplished by microprobe monoion technology Ion Beam Induced Charge (IBIC). After irradiation created areas of selective damage in the diamond detector, low-current mode IBIC microscopy was carried out to measure the degradation of charge collection efficiency (CCE). To gain a better understanding of the detector performance after irradiation, different ions within the ranges of less than, equal to, and greater than the damage layer extension are utilized as IBIC probes. The same irradiation and IBIC microscopy experimental procedures were conducted on detector-grade silicon PIN diodes to directly compare the radiation hardness of diamond and silicon.

The results indicate that single-crystal CVD diamonds have lower radiation hardness for short-range heavy ion spectra compared to high-resistivity silicon, which is contrary to the results obtained from diamond detectors exposed to high-energy particles (**Figure 9**) [23].

To enhance the radiation damage resistance of single-crystal CVD diamond detectors, it has been reported that when a standard (1–10 V/μm) electric field is applied [24], the signal amplitude can be nearly fully restored in a diamond detector that has suffered severe radiation damage, and the defect concentration level of the damaging ions has no effect whatsoever. In addition, it has been demonstrated that increasing the electric field also improves the signal-to-noise ratio (**Figure 10**). Finally, it has been observed that the generation energy of electron-hole pairs decreases slightly as the electric field increases. Although these findings were obtained from relatively

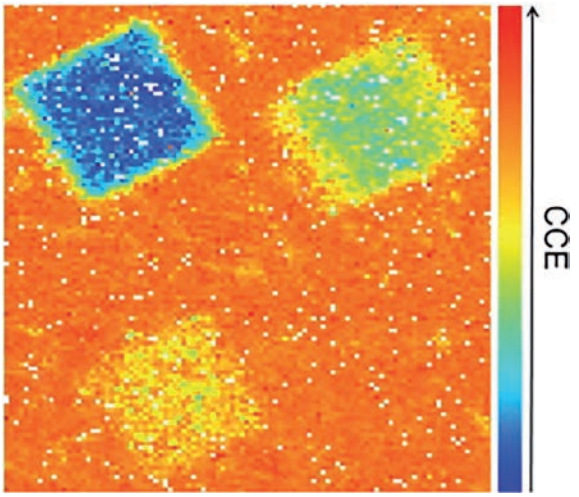


Figure 9.
IBIC pulse height two-dimensional distribution measured using a 430 keV proton probe scanned over the selectively-irradiated diamond detector with a 6.5 MeV carbon micro-beam. The bias voltage applied to the diamond detector is −500 V. Three damaged regions corresponding to the lower CCE are clearly observable [23]. Copyright 2013, Elsevier, used with permission of the publisher.

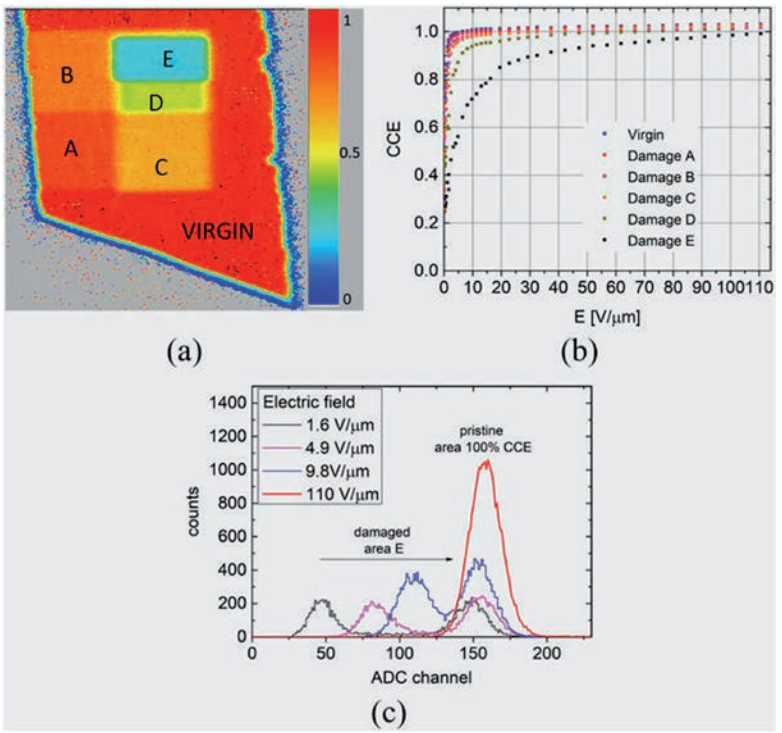


Figure 10.
(a) Map of the damaged and undamaged areas of the detector irradiated with a 26-MeV oxygen beam at an electric field of 10 V/μm. (b) Plots of CCE versus electric field for five distinct damaged areas and the undamaged part of the detector using a 2-MeV proton beam. (c) Ion Beam Induced Charge (IBIC) pulse-height spectra of the undamaged and "E" damaged areas at E = 1.6, 4.9, 9.8, 110 V/μm (refer to the text for selection criteria). Copyright 2019, The Authors, published by AIP, used with permission of the publisher.

small detector volumes, the advantages of high electric fields are evident and offer new perspectives on potential applications as hard detectors for extreme radiation in high-energy physics experiments or under other extremely high-radiation conditions (e.g., fusion reactors).

5. Effect of neutron irradiation

The detection of neutrons across a wide spectrum holds great significance in nuclear physics and nuclear data measurement. Some scholars have investigated the performance of diamond detectors under the irradiation of wide-spectrum neutrons [25]. By extracting and analyzing key parameters such as pulse width and count rate, a technical procedure is presented for assessing the stability of diamond radiation detectors in complex radiation fields (**Figure 11**).

Neutron diagnosis is a crucial component of fusion diagnosis, and certain scholars have reported the relevant performance parameters of diamond detectors irradiated by 14.8 MeV energy neutrons. The energy resolution falls within the range of 20 KeV FWHM. The lifetime of diamond under neutron irradiation is extrapolated to 10^{15} n/cm^2 at a 30% degradation level. It exhibits high-temperature compatibility, with stable operation up to 250°C for e^- -and h^+-readout, and a 12% reduction in response up to 500°C for readout. In addition, some scholars have installed a single-crystal diamond

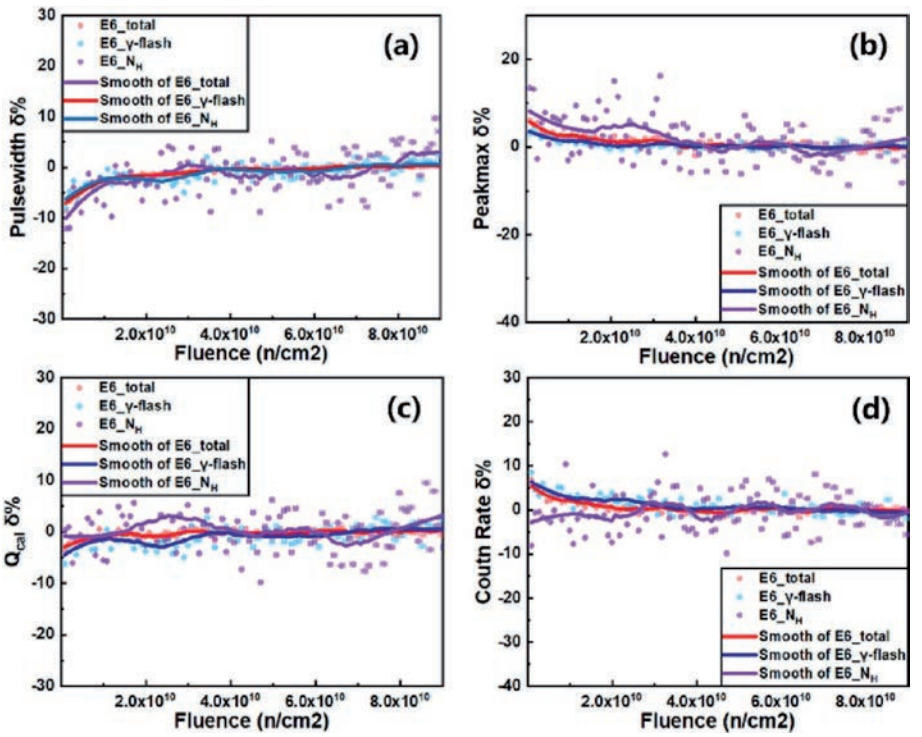


Figure 11.
The relationship between the fluence and (a) Pulse width, (b) Peak maximum, (c) Qcal, (d) count rate of the diamond detector under −400 V at Back-n. The vertical axis represents the variation rate δ of parameters relative to stable values. Total, γ-Flash, and NH are denoted in red, blue, and purple, respectively [25]. Copyright 2024, Elsevier, used with permission of the publisher.

detector in a large spiral device for high-energy ion detection. The D-T neutron measurement results indicate that the energy resolution of 14 MeV neutrons is 1.7%, which is adequate for measuring the fuel ion temperature in fusion - combustion plasma.

5.1 Nuclear batteries

A diamond nuclear battery is a device that harnesses the energy produced by the decay of radioactive isotopes and directly converts it into electricity via semiconductor materials, specifically synthetic diamonds in this instance. This power generation process involves no chain reaction, poses no risk of explosion, and has virtually no risk of nuclear radiation leakage. It can effectively address issues such as nuclear waste utilization, clean power generation, and battery lifespan. Batteries typically select radioactive isotopes that emit low-energy beta (β) particles. The most common ones are nickel-63 or tritium, and there are also studies on carbon-14 extracted from nuclear waste. β particles are high-speed electrons with weak penetration, which renders the battery highly safe. The core structure of the battery is a p-n junction. The radioactive isotope (nickel-63) is implanted or placed in a diamond semiconductor layer that continuously emits β particles in all directions. When the β particles strike the atoms of the diamond semiconductor material, they generate electron - hole pairs. The built - in electric field within the p-n junction separates the electrons from the hole pairs. When the p-n junction is connected with wires, these separated electrons flow through the external circuit to the P-type region and recombine with the holes, thus creating a continuous current. Some scholars have studied the energy response of diamond semiconductors to B radiation, which is of great significance to the study of diamond nuclear batteries [26]. The research team used CVD single crystal diamonds measuring 4.5 × 4.5 and 0.5 mm thick, and deposited titanium/palladium metal electrodes on both sides of the diamond. The current-voltage curve of this structure (from −400 to 400 V in steps of 25 V), as shown in **Figure 12**, shows that this sensor is ohmic when the voltage is between 100 V to about 300 V.

The study employed three radiation sources: ^{147}Pm, ^{204}Tl, and ^{90}Sr/^{90}Y for β particle measurements. The range of beta particles in diamonds from ^{147}Pm is less than the thickness of the diamond chip, yet some betas from ^{204}Tl and ^{90}Sr/^{90}Y have a range greater than the thickness of the diamonds (**Figure 13**). The study indicates that diamond detectors exhibit a particularly sensitive response to β radiation. Owing

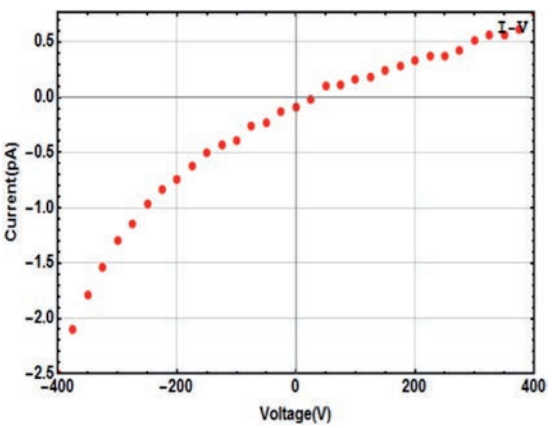


Figure 12.
Current-voltage measurement. Copyright 2018, Elsevier, used with permission of the publisher.

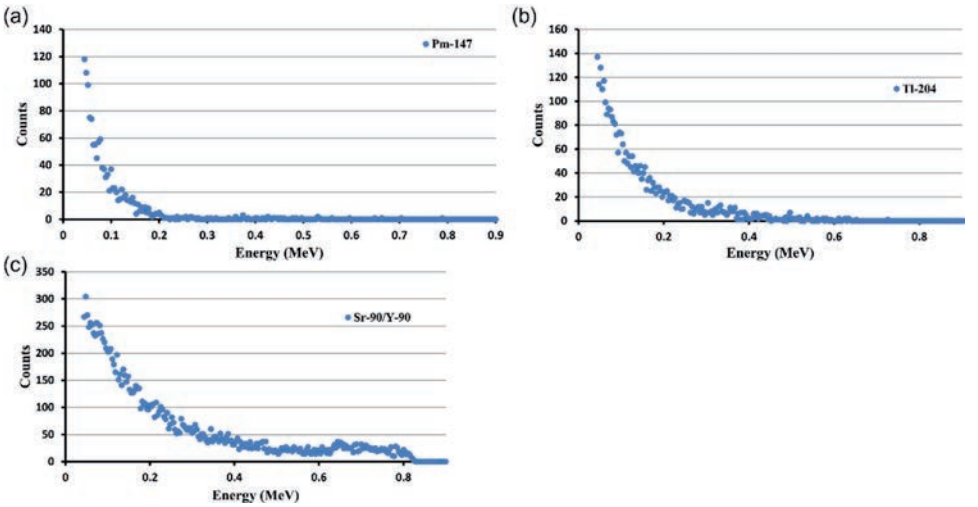


Figure 13.
Energy response spectrum of diamond sensors. (a) Energy spectrum of 147Pm detected by the diamond sensor. (b) Energy spectrum of ^{204}Tl detected by the diamond sensor. (c) Energy spectrum of $^{90}Sr/^{90}Y$ detected by the diamond sensor. Copyright 2018, Elsevier, used with permission of the publisher.

to the limited thickness of synthetic electronic-grade diamonds, the sensitivity of the detectors can be enhanced by splicing diamond chips for higher-energy β radiation. Although this study did not construct p-n junctions, it holds significant value for the selection of radiation source energy in diamond nuclear cells.

In 2015, Vitaly B et al. first reported a large area diamond nuclear cell prototype and investigated its performance under different radioactive sources [27]. The typical energy conversion efficiency of 130 Schottky barrier diamond diodes employed in battery modules is approximately 5%. The conclusions derived from different radiation sources indicate that the structural size of Schottky barrier diamond diodes is vital for enhancing the utilization of radiation energy, as presented in **Table 1**. It also contributes to improving the service life of the diode and safeguarding the crystal lattice structure.

Subsequently, the team successfully separated the CVD layer from the HPHT diamond substrate by means of ion implantation-assisted stripping technology to fabricate ultra-thin diamond conversion cells [28]. By alternating the polarity in parallel between 2 μm thin diamond-based conversion cells and 200 μm thick cells with opposite polarity, a single vertical stack was obtained (**Figure 14**). The proposed diamond core battery featuring a 3D structure offers a total output power of 0.93 μW and a power density of approximately 3300 mWh/g, which is an order of magnitude higher than that of the previous structure.

Isotope	OC voltage	SC current	Output power	Efficiency
^{63}Ni	1.68 V	55 nA	45 nW	0.6%
^{147}Pm	1.81 V	2.4 μA	2.4 μW	1%
$^{90}Sr/^{90}Y$	1.75 V	510 nA	0.55 μW	0.004%
^{238}Pu	1.85 V	37 μA	36 μW	3.6%

Table 1.
Summarized results of the investigation on the fabricated battery.

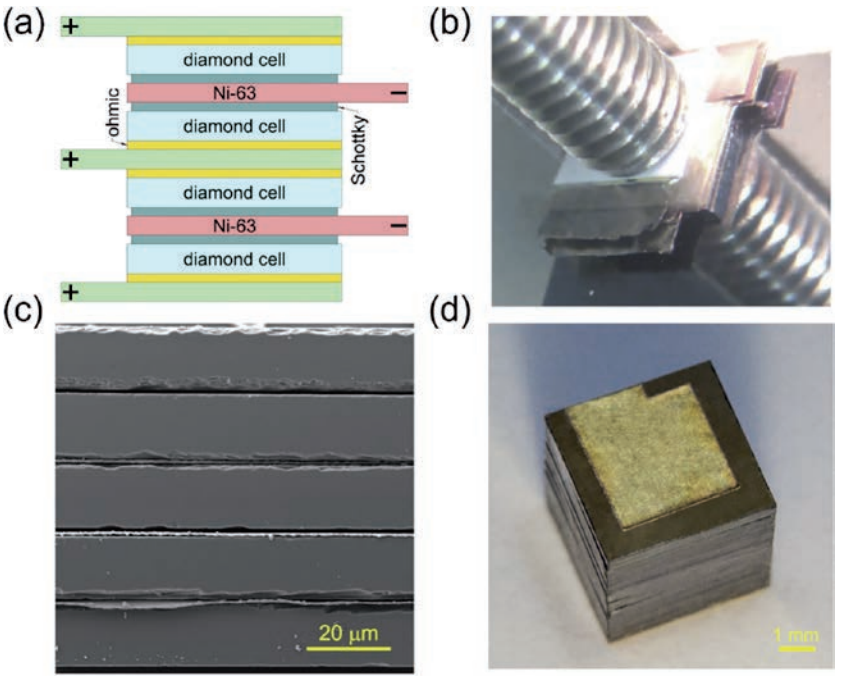


Figure 14.
(a) Cell package: Schematic diagram, (b) Assembly, (c) SEM image of the cross-section, (d) Photograph of the assembled battery. Copyright 2018, Elsevier, used with permission of the publisher.

In 2018, Our team fabricated a diamond Schottky alpha nuclear battery (DSAB) and performed an alpha particle degradation test. As depicted in **Figure 15** [29], CVD intrinsic layer growth was conducted on boron-doped high-temperature and high-pressure diamonds. The impact of hydrogen/oxygen terminals on the open-circuit voltage of DSAB was investigated. It was concluded that oxygen terminals are more suitable for diamond photovoltaic devices than hydrogen terminals. Moreover, DSAB exhibits better stability in open-circuit voltage and short-circuit current compared to silicon and silicon carbide diodes.

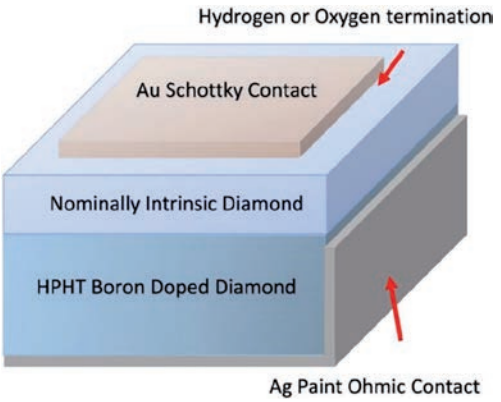


Figure 15.
Structure of the PIM diamond Schottky diode. Copyright 2018, Elsevier, used with permission of the publisher.

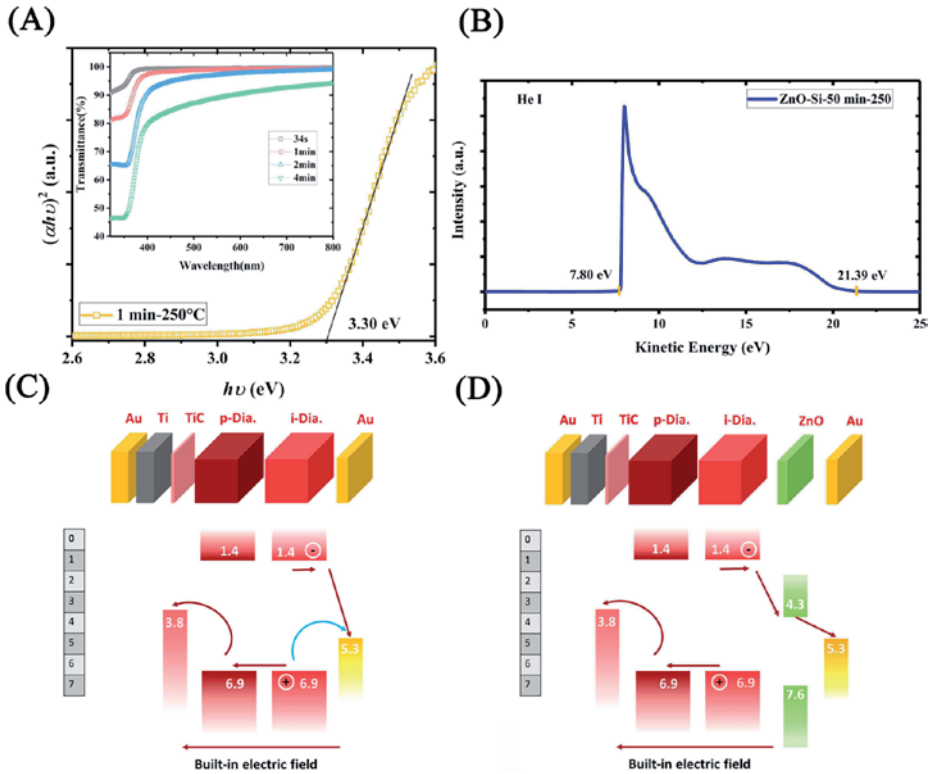


Figure 16.
(a) Tauc plot of the ZnO layer deposited on glass. Inset: UV–Vis transmission spectra of ZnO with varying deposition times. (b) UPS spectrum of the ZnO layer on a silicon substrate. A sample bias of −5 V was applied to observe the secondary electron cutoff (SEC). He I (hυ = 21.22 eV) was utilized. The kinetic energy on the x - axis represents the kinetic energy of the electrons excited by ultraviolet light relative to the Fermi level of the sample and the instrument. Band diagrams of the devices without (c) and with (d) the ZnO layer [30]. Copyright 2020, Elsevier, used with permission of the publisher.

To enhance the open-circuit voltage of diamond nuclear batteries, our team later proposed using a zinc oxide film as the electron transport layer of diamond Schottky nuclear batteries, as depicted in **Figure 16** [30]. The open-circuit voltage of devices equipped with an electron transport layer is 1.43 V, which is 0.4 V higher than that of devices without an electron transport layer. Moreover, the conversion efficiency of the devices has increased by 100% to 1.42%, offering a new approach to improving the open-circuit voltage and conversion efficiency of diamond nuclear batteries.

Overall, diamond nuclear batteries open up a completely new realm of power supply: ultra-long-life, utterly stable, maintenance-free micro power supplies. They have great potential to provide power for special fields such as deep space detectors and pacemakers. However, enhancing the power and conversion efficiency of diamond nuclear batteries still requires researchers to continue to engage in in-depth exploration.

6. Conclusion

Diamond radiation detectors have emerged as the preferred choice for radiation detection in extreme environments, thanks to their exceptional physicochemical

properties and innovative device designs. From a material engineering standpoint, the quality of single crystal diamond substrates is continuously improving, and nanostructure and heterogeneous integration technologies are driving performance breakthroughs. In terms of detection capabilities, remarkable progress has been achieved in high-temperature deep ultraviolet, X/γ-ray, and particle detection. Regarding environmental adaptability, they exhibit unparalleled advantages under extreme conditions such as high temperature, intense radiation, low temperature, and low pressure. In the aspect of application scope, they have expanded into key fields like nuclear safety, aerospace, and biomedicine. Currently, the research frontiers are actively progressing towards large-area arrays, multispectral fusion, quantum limit detection, and new material systems. Despite facing challenges in cost control, doping processes, and large-area uniform growth, diamond detectors are anticipated to achieve broader application breakthroughs by 2030 as CVD technology matures and nanoengineering advances. Particularly in areas of major national requirements, such as nuclear power plant safety monitoring, deep space exploration, and quantum information technology, diamond radiation detectors will play an irreplaceable and crucial role, providing powerful tools for humanity's exploration of extreme environments and cutting-edge science.

Acknowledgements

This work was supported by the National MCF Energy R&D Program of China, grant no. 2019YFE03100200, the National Key R&D Program of China (Grant No. 2023YFB3811700, Grant No. 2022YFE0110900); the National Natural Science Foundation of China (Grant No. 52302040); the China Postdoctoral Science Foundation (Grant No. 2025 T181141, Grant No. 2023 M730840); the Science Foundation of National Key Laboratory of Science and Technology on Advanced Composites in Special Environments (Grant No. JCKYS2024603C006); Funding for the "New Era Longjiang Excellent Master's and Doctoral Dissertations" project (Grant No. LJYXL2023-026); Heilongjiang Postdoctoral Foundation (Grant No. LBH-Z23160); the Research Startup Fund for Youth Top-notch Talents at Harbin Institute of Technology.

Author details

YunPeng Yang[1,2†], Sen Zhang[1,2†], Benjian Liu[1,2*], Zuanquan Chen[1,2], Rui Fan[1,2], Chao Chen[1,2], Linlin Liu[1,2], Wensi Yang[1,2], Binyu Niu[1,2], Rui Chen[1,2], Tao Li[1,2], Kang Liu[1,2,3], Bing Dai[1,2,3] and Jiaqi Zhu[1,2,3]

1 National Key Laboratory of Science and Technology on Advanced Composites in Special Environments, Harbin Institute of Technology, Harbin, P.R. China

2 Zhengzhou Research Institute, Harbin Institute of Technology, Zhengzhou, China

3 Key Laboratory of Micro-systems and Micro-structures Manufacturing, Ministry of Education, Harbin, P.R. China

*Address all correspondence to: liubenjian@hit.edu.cn

† YunPeng Yang and Sen Zhang contributed equally.

IntechOpen

© 2026 The Author(s). Licensee IntechOpen. This chapter is distributed under the terms of the Creative Commons Attribution License (http://creativecommons.org/licenses/by/4.0), which permits unrestricted use, distribution, and reproduction in any medium, provided the original work is properly cited. CC BY

References

[1] Watkins RJ, Salter PS, Moors RJ, Jackman RB. Three-dimensional diamond planar spiral detectors. Scientific Reports. 2025;**15**:8496

[2] Angelone M et al. Development of single crystal diamond neutron detectors and test at JET tokamak. Nuclear Instruments and Methods in Physics Research Section A: Accelerators, Spectrometers, Detectors and Associated Equipment. 2008;**595**:616-622

[3] Shimaoka T et al. High-performance diamond radiation detectors produced by lift-off method. Europhysics Letters. 2016;**113**:62001

[4] Mu L et al. Comparative of HPHT and CVD diamond: Performance and defect analysis for alpha radiation detector. Functional Diamond. 2023;**3**:2271510

[5] Lu J et al. Single-crystal diamond nanowires embedded with platinum nanoparticles for high-temperature solar-blind photodetector. Nano-Micro Letters. 2025;**17**:220

[6] Lin C-N et al. High performance diamond-based solar-blind photodetectors enabled by Schottky barrier modulation. Carbon. 2022;**200**:510-516

[7] Dou W et al. Highly sensitive diamond X-ray detector array for high-temperature applications. Chip. 2024;**3**:100106

[8] Su K et al. A large gain and high resolution diamond radiation detector with Au/hydrogen termination Ohmic contact. IEEE Electron Device Letters. 2022;**43**:454-457

[9] Yu X et al. 1.26 W/mm output power density at 10 GHz for Si3N4 passivated H-terminated diamond MOSFETs. IEEE Transactions on Electron Devices. 2021;**68**:5068-5072

[10] Imanishi S et al. Drain current density over 1.1 a/mm in 2D hole gas diamond MOSFETs with regrown p++-diamond Ohmic contacts. IEEE Electron Device Letters. 2021;**42**:204-207

[11] Wang L et al. High-performance oxygen terminated synthetic single crystal diamond detector for high gamma dose rate measurement. Radiation Measurements. 2024;**177**:107256

[12] Li FN, Li Y, Fan DY, Wang HX. Barrier heights of Au, Pt, Pd, Ir, Cu on nitrogen terminated (1 0 0) diamond determined by X-ray photoelectron spectroscopy. Applied Surface Science. 2018;**456**:532-537

[13] Kono S et al. Direct determination of the barrier height of Au ohmic-contact on a hydrogen-terminated diamond (001) surface. Diamond and Related Materials. 2017;**73**:182-189

[14] Galbiati A et al. IEEE Nuclear Science Symposium Conference Record. Dresden, Germany: IEEE Nuclear and Plasma Sciences Society; 2008. pp. 190-196

[15] Angelone M, Verona C. Properties of diamond-based neutron detectors operated in harsh environments. Journal of Nuclear Engineering. 2021;**2**:422-470

[16] Ogawa K et al. Fusion product diagnostics based on commercially available chemical vapor deposition diamond detector in large helical device. Journal of Instrumentation. 2023;**18**:P01022

[17] Tamaki S, Murata I, Osakabe M. Application of a single crystal CVD diamond detector for fast neutron measurement in high dose and mixed radiation fields. In: 2024 IEEE International Conference on Consumer Electronics (ICCE); 6-8 Jan. 2024; Las Vegas, NV, USA. New York, NY, USA: IEEE; 2024. pp. 1-4

[18] Passeri M et al. Assessment of single crystal diamond detector radiation hardness to 14 MeV neutrons. Nuclear Instruments and Methods in Physics Research Section A: Accelerators, Spectrometers, Detectors and Associated Equipment. 2021;**1010**:165574

[19] Philip O, Gicquel F, Ernst V, Zhou Z. Development and test of a diamond-based fast neutron detector for 200 °C operation. IEEE Transactions on Nuclear Science. 2017;**64**:2683-2689

[20] Cosic D, Provatas G, Jakšić M, Begušić D. Charge collection efficiency of scCVD diamond detectors at low temperatures. Diamond and Related Materials. 2022;**127**:109184

[21] Serpente V et al. X-ray and electrical characterization of a multipixel diamond-based detector in high temperature environments. Diamond and Related Materials. 2023;**135**:109819

[22] Angelone M, Cesaroni S, Loreti S, Pagano G, Pillon M. High temperature response of a single crystal CVD diamond detector operated in current mode. Nuclear Instruments and Methods in Physics Research Section A: Accelerators, Spectrometers, Detectors and Associated Equipment. 2019;**943**:162493

[23] Zamboni I, Pastuović Ž, Jakšić M. Radiation hardness of single crystal CVD diamond detector tested with MeV energy ions. Diamond and Related Materials. 2013;**31**:65-71

[24] Skukan N, Sudić I, Pomorski M, Kada W, Jakšić M. Enhanced radiation hardness and signal recovery in thin diamond detectors. AIP Advances. 2019;**9**(2):025134

[25] Niu M et al. Characterization of a diamond detector during experiments under wide energy spectrum neutrons. Diamond and Related Materials. 2024;**145**:111112

[26] Tchouaso MT, Kasiwattanawut H, Prelas MA. Energy response of diamond sensor to beta radiation. Applied Radiation and Isotopes. 2018;**139**:66-69

[27] Bormashov V et al. Development of nuclear microbattery prototype based on Schottky barrier diamond diodes. Physica Status Solidi (a). 2015;**212**:2539-2547

[28] Bormashov VS et al. High power density nuclear battery prototype based on diamond Schottky diodes. Diamond and Related Materials. 2018;**84**:41-47

[29] Liu B et al. Alpha-voltaic battery on diamond Schottky barrier diode. Diamond and Related Materials. 2018;**87**:35-42

[30] Liu B et al. Enhanced performance of diamond Schottky nuclear batteries by using ZnO as electron transport layer. Diamond and Related Materials. 2020;**109**:108026